View metadata, citation and similar papers at core.ac.uk
brought to you by CORE
provided by Digital.CSIC

Lignin Composition and Structure in Young versus Adult *Eucalyptus globulus* Plants[1]

Jorge Rencoret, Ana Gutiérrez, Lidia Nieto, J. Jiménez-Barbero, Craig B. Faulds, Hoon Kim, John Ralph, Ángel T. Martínez, and José C. del Río*

Instituto de Recursos Naturales y Agrobiología de Sevilla, Consejo Superior de Investigaciones Científicas, E–41080 Seville, Spain (J. Rencoret, A.G., J.C.d.R.); Centro de Investigaciones Biológicas, Consejo Superior de Investigaciones Científicas, E–28040 Madrid, Spain (L.N., J.J.-B., C.B.F., A.T.M.); and Departments of Biochemistry and Biological Systems Engineering and Department of Energy Great Lakes Bioenergy Research Center, University of Wisconsin, Madison, Wisconsin 53706 (J. Rencoret, H.K., J. Ralph)

Lignin changes during plant growth were investigated in a selected *Eucalyptus globulus* clone. The lignin composition and structure were studied in situ by a new procedure enabling the acquisition of two-dimensional nuclear magnetic resonance (2D-NMR) spectra on wood gels formed in the NMR tube as well as by analytical pyrolysis-gas chromatography-mass spectrometry. In addition, milled-wood lignins were isolated and analyzed by 2D-NMR, pyrolysis-gas chromatography-mass spectrometry, and thioacidolysis. The data indicated that *p*-hydroxyphenyl and guaiacyl units are deposited at the earlier stages, whereas the woods are enriched in syringyl (S) lignin during late lignification. Wood 2D-NMR showed that β-*O*-4′ and resinol linkages were predominant in the eucalypt lignin, whereas other substructures were present in much lower amounts. Interestingly, open β-1′ structures could be detected in the isolated lignins. Phenylcoumarans and cinnamyl end groups were depleted with age, spirodienone abundance increased, and the main substructures (β-*O*-4′ and resinols) were scarcely modified. Thioacidolysis revealed a higher predominance of S units in the ether-linked lignin than in the total lignin and, in agreement with NMR, also indicated that resinols are the most important nonether linkages. Dimer analysis showed that most of the resinol-type structures comprised two S units (syringaresinol), the crossed guaiacyl-S resinol appearing as a minor substructure and pinoresinol being totally absent. Changes in hemicelluloses were also shown by the 2D-NMR spectra of the wood gels without polysaccharide isolation. These include decreases of methyl galacturonosyl, arabinosyl, and galactosyl (anomeric) signals, assigned to pectin and related neutral polysaccharides, and increases of xylosyl (which are approximately 50% acetylated) and 4-*O*-methylglucuronosyl signals.

Plant cell walls are composed mainly of three structural polymers, the carbohydrates cellulose and the hemicelluloses and the aromatic polymer lignin. The lignin polymer provides mechanical support to the plant. In addition, it waterproofs the cell wall, enabling transport of water and solutes through the vascular system, and plays a role in protecting plants against pathogens. Lignin is a complex polymer synthesized mainly from three hydroxycinnamyl alcohols differing in their degree of methoxylation: *p*-coumaryl, coniferyl, and sinapyl alcohols (Higuchi, 1997; Boerjan et al., 2003; Ralph et al., 2004a). Each of these monolignols gives rise to a different type of lignin unit called *p*-hydroxyphenyl (H), guaiacyl (G), and syringyl (S) units, respectively, when incorporated into the polymer. The amount and composition of lignins vary among taxa, cell types, and individual cell wall layers and also with environmental conditions. Softwood lignin consists almost exclusively of G-type lignin, while hardwood lignin also consists of S units (H units being minor components). After their synthesis, the lignin monomers are transported to the cell wall, where they are polymerized in a combinatorial fashion by free radical coupling mechanisms in a reaction mediated by peroxidases and/or laccases, generating a variety of structures and linkages within the polymer (Boerjan et al., 2003; Ralph et al., 2004a). Wood (secondary xylem) is produced seasonally at the periphery of the trunk by the vascular cambium (Déjardin et al., 2010). Lignin deposition is one of the final stages of xylem cell differentiation and mainly takes place during secondary thickening of the cell wall. Lignification starts in the middle lamella and cell corners and proceeds toward the lumen, filling up pores in the already deposited polysaccharide network (Donaldson, 2001; Boerjan et al., 2003). The relative abundance of the different linkages formed depends on the relative

[1] This study was supported by the Spanish project AGL2005–01748, the Consejo Superior de Investigaciones Científicas (project nos. 200640I039 and 201040E075), the European Union projects BIORENEW (grant no. NMP2–CT–2006–026456), WALLESTER (grant no. PIEF–GA–2009–235938), and LIGNODECO (grant no. KBBE–244362), the Department of Energy Great Lakes Bioenergy Research Center (grant no. BER DE–FC02–07ER64494), and the Spanish Ministry of Education (postdoctoral fellowship to J. Rencoret).

* Corresponding author; e-mail delrio@irnase.csic.es.

The author responsible for distribution of materials integral to the findings presented in this article in accordance with the policy described in the Instructions for Authors (www.plantphysiol.org) is: José C. del Río (delrio@irnase.csic.es).

www.plantphysiol.org/cgi/doi/10.1104/pp.110.167254

contribution of the particular monomers to the polymerization process as well as on steric hindrances and chemical interactions in the growing wall. Therefore, the differences in the timing of monolignol deposition and the changes in cell wall ultrastructure during growth would regulate lignin composition and structure during lignification.

A main challenge in elucidating the structure of lignins is in obtaining high-yield isolation from wood in a chemically unaltered form (the same applies to hemicellulose polysaccharides). Several lignin isolation procedures have been developed, but it is well recognized that the different procedures, including the reference milled-wood lignin (MWL), yield only a part of the native lignin in wood and may not be representative of the whole lignin. Indeed, it has also been demonstrated that MWL can undergo some structural modifications during isolation, especially during the milling process, and often contains some amount of "contaminating" compounds (such as lignin-linked carbohydrates; Fujimoto et al., 2005; Guerra et al., 2006; Hu et al., 2006; Balakshin et al., 2008). Because lignin is intimately interpenetrating the other major components (cellulose and hemicelluloses), it is obvious that its truly native form can only be studied by analytical methods applicable directly on the whole plant material. For this purpose, in this paper, the wood samples were analyzed in situ by two-dimensional (2D)-NMR spectroscopy and pyrolysis-gas chromatography-mass spectrometry (Py-GC-MS). The use of these techniques avoids isolation procedures that may lead to partial or modified polymer extraction. For in situ NMR analyses, a recent approach has been developed that consists of swelling finely ground plant material in deuterated dimethyl sulfoxide (DMSO-d_6; Kim et al., 2008; Rencoret et al., 2009) or DMSO-d_6:pyridine-d_5 (4:1; Kim and Ralph, 2010) and forming a gel directly in the NMR tube, which is readily amenable to NMR analysis. Heteronuclear single quantum correlation (HSQC) NMR of these gels has been shown to be an efficient method for the rapid in situ analysis of lignin in plants without the need of prior isolation. The method requires only low amounts of sample and can be used for rapid characterization of the major structural features of plant lignins (i.e. interunit linkages and H-G-S composition), also providing information on the hemicellulose polysaccharides. Py-GC-MS is another powerful tool for the in situ characterization of plant constituents, especially lignin (Ralph and Hatfield, 1991; Rodrigues et al., 1999; del Río et al., 2005; Rencoret et al., 2007). Wood lignin is pyrolyzed to produce a mixture of relatively simple phenols, which result from cleavage of ether and certain carbon-carbon linkages. These phenols retain their substitution patterns from the lignin polymer, and it is thus possible to identify compounds from the H, G, and S lignin units.

The aim of this paper is to elucidate the changes produced in the composition and structure of the lignin in eucalypt wood with maturation and includes analyses of young plants and adult trees. This knowledge is important not only for providing additional insight into the mechanisms of lignin deposition but also for the industrial processing of wood for pulp, chemical, or biofuel production, as the lignin composition and structure greatly influence the delignification reactions (González-Vila et al., 1999; del Río et al., 2005). For this purpose, samples of *Eucalyptus globulus* wood from the same clone (to avoid genetic variations within species) were collected at different stages of growth (1 month, 18 months, and 9 years) and the composition and structure of their lignins were thoroughly investigated. A combination of the abovementioned 2D-NMR and Py-GC-MS of whole wood samples was used for the in situ study of lignin changes. In order to obtain further insights into their structures and compare with the results from the in situ analyses, MWL was also isolated from the different woods and analyzed by NMR, pyrolysis, and thioacidolysis. As far as we know, this is the first report describing in situ structural analyses of wood lignin during tree growth using a combination of 2D-NMR and other techniques.

RESULTS AND DISCUSSION

After a general analysis of wood composition in *E. globulus* plants of different ages (young and adult trees from a clonal plantation), the changes in lignin (and hemicellulose) during growth were analyzed in situ by a combination of Py-GC-MS and 2D-NMR of whole wood, and the results were compared (and complemented) with those obtained from lignins (MWL) isolated from the same samples.

Wood Composition during Eucalypt Growth

The contents of the main wood constituents (i.e. acetone extractives, water-soluble material, Klason lignin, acid-soluble lignin, crystalline cellulose, amorphous glucan, xylan, arabinan, galactan, mannan, rhamnan, fucan, total uronic acids, and ash) in the selected *E. globulus* clone at different stages of growth are summarized in Table I. The total lignin content (Klason lignin plus acid-soluble lignin) increased during growth (from 16% in the 1-month-old sample to 25% in the 9-year-old wood), whereas the content of other constituents (namely acetone extractives, water-soluble material, and ash) decreased with maturity. Interestingly, there is also a great variation in the composition of polysaccharides (from neutral sugar analysis) during maturation, with a depletion of Ara, Gal, and Man and a progressive enrichment of Xyl. The amount of crystalline cellulose has the highest content (37%) after 18 months, while that of amorphous glucan was lower and showed a progressive increase during growth. Finally, the uronic acid content was the highest after 1 month (7%) and showed only a moderate decrease during growth. Variations in the uronic acid nature

Table I. *Abundances (%) of the main constituents of E. globulus wood at different growth stages*

Constituents	1 Month	18 Months	9 Years
Acetone extractives	8.6	0.5	0.6
Water-soluble extracts	6.6	1.4	2.2
Klason lignin	13.0	17.5	19.8
Acid-soluble lignin	2.7	5.2	4.7
Cellulose (crystalline)	25.0	36.7	29.9
Glucan (amorphous)	11.4	15.0	16.2
Xylan	12.2	14.0	17.1
Arabinan	3.8	0.9	0.8
Galactan	2.7	1.2	1.5
Mannan	0.9	0.4	0.4
Rhamnan	0.7	0.4	0.5
Fucan	0.3	0.1	0.1
Uronic acids	7.4	5.9	5.8
Ash	4.6	0.7	0.4

during growth are discussed after the NMR analyses below.

Py-GC-MS of Whole Woods and Their Isolated Lignins

Py-GC-MS, although not a fully quantitative technique, has been successfully used to analyze the relative H-G-S composition of lignin in different hardwoods, including eucalypt wood (Rodrigues et al., 1999; Yokoi et al., 1999, 2001; del Río et al., 2005; Rencoret et al., 2007, 2008). Pyrograms from the eucalypt wood samples after different growth periods and their corresponding MWLs are shown in Figures 1 and 2, and the identities and relative molar abundances of the released lignin-derived compounds are listed in Table II.

The pyrolysis of the different eucalypt woods released both carbohydrate- and lignin-derived compounds. Among the latter, guaiacol- and syringol-type phenols, derived from the G and S lignin units, were identified, including guaiacol (compound 2), 4-vinylguaiacol (8), syringol (11), 4-methylsyringol (14), 4-vinylsyringol (22), 4-allylsyringol (25), trans-4-propenylsyringol (32), syringaldehyde (34), and trans-sinapaldehyde (49). In addition, significant amounts of compounds derived from H lignin units, such as phenol (1), methylphenols (3 and 4), and dimethylphenol (6), could be detected after pyrolysis of the youngest wood, although some of them can also derive from polysaccharides (Ralph and Hatfield, 1991). The H-G-S composition of the lignin in the different woods, obtained from the molar areas of all the lignin-derived compounds, is shown in Table II. In all samples, the S-type phenols were released in higher abundances than the respective G-type phenols, with a S-G ratio ranging from 1.4 in the youngest wood to 3.8 in the oldest wood. The amount of H-type compounds from the youngest wood (9%) decreases during maturation (to only 2% in the oldest wood). This indicates that H units are deposited first, followed by G and then S units, in agreement with previous microautoradiography and microspectroscopy studies in other plants (Terashima et al., 1986). An increase of lignin S-G ratio with plant maturity has also been reported after Py-GC-MS of nonwoody fibers (Mazumder et al., 2005). This difference in timing of monolignol deposition would also be responsible for the within-tree variation of the S-G ratio observed in *Eucalyptus camaldulensis* wood (Ona et al., 1997; Yokoi et al., 1999).

Pyrolysis of the MWLs isolated from the different *E. globulus* woods (Fig. 2) released a similar distribution of lignin-derived compounds as from their respective woods, although the content of H units was lower (Table II). This is especially evident in the case of the MWL isolated from the 1-month-old wood. However, we must note that MWL may reflect only the most accessible part of the native lignin in the plant, which may be depleted in highly condensed H lignin units. In any case, the same trend observed in the pyrolysis of woods, which indicates an increase of S lignin units and a decrease of H and G lignin units with maturity, was also observed in the pyrolysis products of MWL, supporting the in situ analysis and confirming a monolignol deposition order of H, G, and then S during *E. globulus* lignification.

2D-NMR of Wood Gels and Their Isolated Lignins

The eucalypt wood samples from different growing periods were analyzed by 2D-NMR (in the gel state) to overcome the drawbacks associated to polymer isolation, namely low yield and artifact formation, and the spectra were compared with those from the lignins (MWL) isolated from the same woods.

The HSQC spectra of the different woods, and their MWLs, are shown in Figures 3 and 4. Carbohydrate signals were predominant in the spectra of the whole wood. They included correlations in the range δ_C/δ_H 60 to 85/2.5 to 5.5, which partially overlapped with lignin signals, and the well-resolved anomeric correlations in the range δ_C/δ_H 90 to 110/3.5 to 6.0. However, lignin signals were also clearly observed in the HSQC spectra, including that of the youngest wood with the lowest lignin content. On the other hand, the spectra of the MWL presented mostly lignin signals that, in general terms, matched those observed in the HSQC spectra of the woods.

Lignin and carbohydrate contours in the HSQC spectra were assigned by comparison with the literature (Ämmälahti et al., 1998; Ralph et al., 1999, 2004b; Capanema et al., 2001, 2004, 2005; Balakshin et al., 2003, 2005; Liitiä et al., 2003; Ha et al., 2005; Golovchenko et al., 2007; Ibarra et al., 2007a, 2007b; del Río et al., 2008, 2009; Kim et al., 2008; Rencoret et al., 2008, 2009; Çetinkol et al., 2010; Kim and Ralph, 2010; Ralph and Landucci, 2010). The main lignin correlation assignments are listed in Table III, and the main lignin substructures found in the different eucalypt woods are depicted in Figure 5. The assignments of the main carbohydrate signals are listed in Table IV.

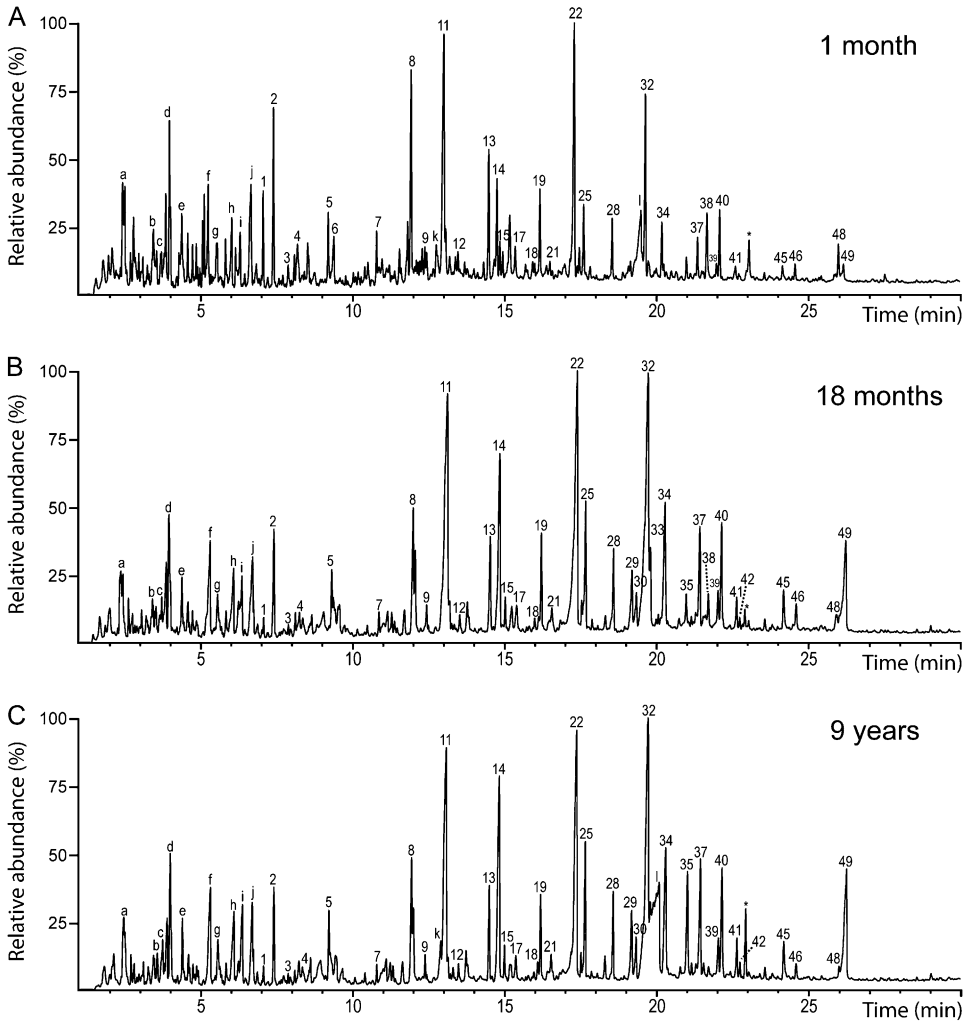

Figure 1. Py-GC-MS chromatogram of the *E. globulus* wood samples at different growth stages. The numbers refer to the lignin-derived compounds, whose identities and relative abundances are listed in Table II. Letters refer to the carbohydrate-derived compounds: a, hydroxyacetaldehyde; b, (*3H*)-furan-2-one; c, (*2H*)-furan-3-one; d, furfural; e, 2-hydroxymethylfuran; f, 2,3-dihydro-5-methylfuran-2-one; g, 5-methyl-2-furfuraldehyde; h, (*5H*)-furan-2-one; i, 4-hydroxy-5,6-dihydro-(*2H*)-pyran-2-one; j, 2-hydroxy-3-methyl-2-cyclopenten-1-one; k, 5-hydroxymethyl-2-furfuraldehyde; l, levoglucosane.

Side Chain Region of the HSQC Spectra: Analysis of Interunit Linkages in Lignin

The side chain region of the spectra gave useful information about the interunit linkages present in lignin. All the spectra showed prominent signals corresponding to *β-O-4′* ether units (substructure A). The C_α-H_α correlations in *β-O-4′* substructures were observed at δ_C/δ_H 71 to 72/4.7 to 4.9 ppm, while the C_β-H_β correlations were observed at δ_C/δ_H 84/4.3 and 86/4.1 ppm for substructures linked to G and S units, respectively. The C_γ-H_γ correlations in *β-O-4′* substructures were observed at δ_C/δ_H 59/3.4 and 3.7 ppm, partially overlapped with other signals. In addition, strong signals for resinol (*β-β′*) substructures (B) were observed in all spectra, with their C_α-H_α, C_β-H_β, and the double C_γ-H_γ correlations at δ_C/δ_H 85/4.7, 54/3.1, and 71/3.8 and 4.2, respectively. Phenylcoumaran (*β-5′*) substructures (C) were also found, although in lower amounts, the signals for their C_α-H_α and C_β-H_β correlations being observed at δ_C/δ_H 87/5.5 and 54/3.5, respectively, and that of the C_γ-H_γ correlation overlapping with other signals around δ_C/δ_H 63/3.7. Finally, small signals corresponding to spirodienone (*β-1′/α-O-α′*) substructures (D) could also be observed in the spectra, their C_α-H_α, $C_{\alpha'}$-$H_{\alpha'}$, C_β-H_β, and $C_{\beta'}$-$H_{\beta'}$ correlations being at δ_C/δ_H 82/5.1, 87/4.4, 60/2.8, and 79/4.1, respectively. Other small signals observed in the side chain region of the HSQC spectra corresponded to C_β-H_β correlations (at δ_C/δ_H 84/5.2) of *β-O-4′* substructures bearing a C_α carbonyl group (F) and the C_γ-H_γ correlation (at δ_C/δ_H 62/4.1) assigned to *p*-hydroxycinnamyl alcohol end groups (I). The HSQC spectra of the isolated MWL also reflected the same side chain signals observed in the spectra of the whole woods, although they were better resolved and some new signals were observed. These included small signals corresponding to C_β-H_β correlations (at δ_C/δ_H 55/2.8) of conventional open *β-1′* substructures (E; Lundquist, 1987) that were observed only in the MWL spectra. Some aliphatic (nonoxygenated) cross-signals appeared in the δ_C/δ_H 10 to 40/0.5 to 2 ppm region (not included in Fig. 4), which were especially abundant in the 1-month sample and could include

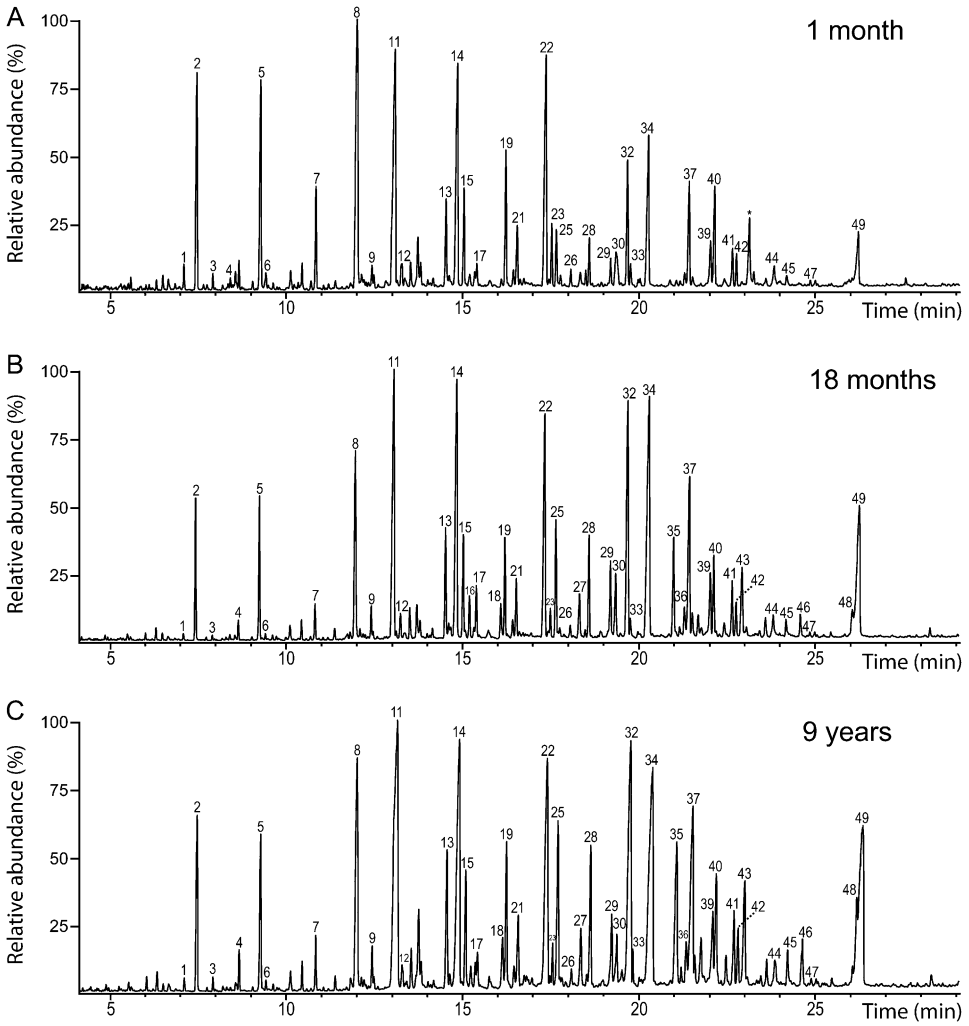

Figure 2. Py-GC-MS chromatogram of the MWLs isolated from the *E. globulus* wood samples at different growth stages. The identities and relative abundances of the released compounds are listed in Table II.

cutin-like material (Deshmukh et al., 2005) or other polymethylenic structures.

Aromatic Region of the HSQC Spectra: Analysis of Lignin Units

The main cross-signals in the aromatic region of the HSQC spectra corresponded to the aromatic rings of the different lignin units. Correlations from S, G, and H lignin units could be observed in the spectra of whole wood and their MWLs. The S lignin units showed a prominent signal for the $C_{2,6}$-$H_{2,6}$ correlation at δ_C/δ_H 104/6.7, while the G units showed different correlations for C_2-H_2 (δ_C/δ_H 111/7.0), C_5-H_5 (δ_C/δ_H 115/6.7 and 7.0), and C_6-H_6 (δ_C/δ_H 119/6.8). Signals corresponding to $C_{2,6}$-$H_{2,6}$ correlations in C_α-oxidized S lignin units (S′) were observed at δ_C/δ_H 107/7.3 and 107/7.2. Signals of H lignin units at δ_C/δ_H 115/6.7 and 128/7.2 for $C_{3,5}$-$H_{3,5}$ and $C_{2,6}$-$H_{2,6}$ respectively, were only detected in the HSQC spectra of the youngest wood sample (1 month), in agreement with the higher presence of H units shown by Py-GC-MS. An extra and well-resolved signal was also detected at δ_C/δ_H 109/7.1 in this sample (in both wood and MWL) that was tentatively assigned to a G-type structure. Olefinic cross-signals of fatty acid structures with one/two double bonds, similar to those from oleic acid (δ_C/δ_H 130/5.3) and linoleic acid (δ_C/δ_H 128/5.3 and 130/5.3), were also identified (Fig. 4). They probably originate from the cutin-like structures mentioned in the previous section. The cross-signal of pyridine used to form the wood gels was also observed (δ_C/δ_H around 124/7.3).

Summary of Changes in Lignin Structure as Revealed by 2D-NMR

The relative abundances of the H, G, and S lignin units, and those of the main interunit linkages (referred to as per 100 aromatic units and as a percentage of the total side chains), calculated from the HSQC spectra of the whole woods and of their respective MWLs, are shown in Table V. The H-G-S composition and the S-G ratio (ranging from 1.2 in the youngest wood to 3.3 in the oldest one) are in close agreement

Table II. *Identification and relative molar abundance (%) of the lignin-derived compounds identified in the Py-GC-MS of E. globulus wood at the different growth stages and from their isolated MWLs*

No.	Compounds	1 Month		18 Months		9 Years	
		Wood	MWL	Wood	MWL	Wood	MWL
1	Phenol	5.5	1.0	0.8	0.2	0.7	0.3
2	Guaiacol	8.7	8.4	4.0	3.6	3.5	3.8
3	Methylphenol	0.9	0.5	0.3	0.1	0.3	0.2
4	Methylphenol	2.7	0.5	0.4	0.1	0.4	0.2
5	4-Methylguaiacol	2.9	7.3	1.7	3.5	2.2	3.0
6	Dimethylphenol	0.3	0.6	0.4	0.2	0.5	0.1
7	4-Ethylguaiacol	1.9	2.6	0.6	0.8	0.5	0.8
8	4-Vinylguaiacol	9.7	10.0	4.5	3.9	4.9	3.3
9	Eugenol	0.9	0.5	0.6	0.6	0.6	0.6
10	Propylguaiacol	0.5	0.2	0.1	0.1	0.1	0.1
11	Syringol	11.8	13.4	14.1	10.7	11.4	13.1
12	cis-Isoeugenol	0.7	0.6	0.5	0.7	0.4	0.6
13	trans-Isoeugenol	5.4	2.3	3.1	2.5	2.7	2.5
14	4-Methylsyringol	3.9	9.0	7.9	9.0	9.6	8.5
15	Vanillin	0.9	2.6	0.7	2.4	0.8	1.9
16	Propynylguaiacol	0.4	0.4	0.5	1.0	0.4	0.4
17	Propynylguaiacol	0.4	0.5	0.6	1.1	0.4	0.5
18	Homovanillin	0.0	0.2	0.3	0.9	0.5	0.9
19	4-Ethylsyringol	2.9	3.2	2.3	1.9	0.2	2.1
20	Vanillic acid methyl ester	0.0	0.3	0.0	0.3	0.0	0.3
21	Acetoguaiacone	0.6	1.6	0.8	1.3	0.6	1.3
22	4-Vinylsyringol	12.6	8.7	14.6	6.6	12.3	6.9
23	Guaiacylacetone	0.8	1.2	0.3	0.5	0.4	0.4
24	Propylsyringol	0.0	0.6	0.0	0.7	0.0	0.8
25	Allylsyringol	2.4	0.4	3.4	1.6	3.5	1.7
26	Propiovanillone	0.1	0.4	0.1	0.3	0.1	0.3
27	Guaiacylvinylketone	0.0	0.4	0.0	1.1	0.0	1.0
28	cis-Propenylsyringol	1.9	1.0	2.1	1.9	1.9	2.0
29	Propynylsyringol	0.5	0.6	1.8	1.7	2.4	1.1
30	Propynylsyringol	0.3	0.4	0.9	1.2	1.1	0.7
31	Vanillic acid	0.0	0.5	0.0	0.2	0.0	0.1
32	trans-Propenylsyringol	6.4	3.0	11.2	6.5	11.4	7.1
33	Dihydroconiferyl alcohol	0.7	0.5	0.9	0.3	0.7	0.3
34	Syringaldehyde	1.8	5.5	4.6	10.4	5.2	9.1
35	Homosyringaldehyde	0.0	0.0	0.7	2.3	3.2	3.1
36	Syringic acid methyl ester	0.1	0.3	0.2	0.6	0.2	0.5
37	Acetosyringone	1.4	2.6	2.6	4.2	3.5	4.3
38	trans-Coniferyl alcohol	3.0	0.0	0.8	0.5	0.3	0.8
39	Coniferaldehyde	0.5	1.3	0.8	1.6	1.1	1.4
40	Syringylacetone	2.2	2.3	2.3	1.4	3.0	1.5
41	Propiosyringone	0.7	0.9	0.7	1.1	0.9	1.0
42	Syringyl-3-oxo-propanal	0.0	0.6	0.0	0.6	0.0	0.7
43	Syringylvinylketone	0.1	0.1	0.2	1.2	0.3	1.1
44	Syringic acid	0.0	0.7	0.0	0.7	0.0	0.5
45	Dihydrosinapyl alcohol	0.6	0.2	1.1	0.4	1.2	0.5
46	cis-Sinapyl alcohol	0.5	0.0	0.6	0.5	0.4	0.7
47	cis-Sinapaldehyde	0.0	0.1	0.1	0.1	0.1	0.1
48	trans-Sinapyl alcohol	1.3	0.0	0.6	0.7	0.3	1.8
49	trans-Sinapaldehyde	0.7	2.0	4.8	6.0	5.7	5.7
Total H		9.4	2.6	1.9	0.7	1.9	0.8
Total G		38.5	42.0	21.2	27.5	20.4	24.3
Total S		52.1	55.4	76.9	71.8	77.6	74.9

with the data obtained by Py-GC-MS, indicating a decrease of H and G units and an increase of S lignin units during lignification. The content of H lignin in the isolated MWL was lower than in the respective wood samples, as already observed by Py-GC-MS.

With respect to the different linkage types, all the lignins showed a predominance of β-*O*-4′ units (A and F; 69%–72% of total side chains) followed by β-β′ resinol-type units (B; 16%–19%) and lower amounts of β-5′ phenylcoumaran-type (C; 1%–5%) and β-1′ spiro-

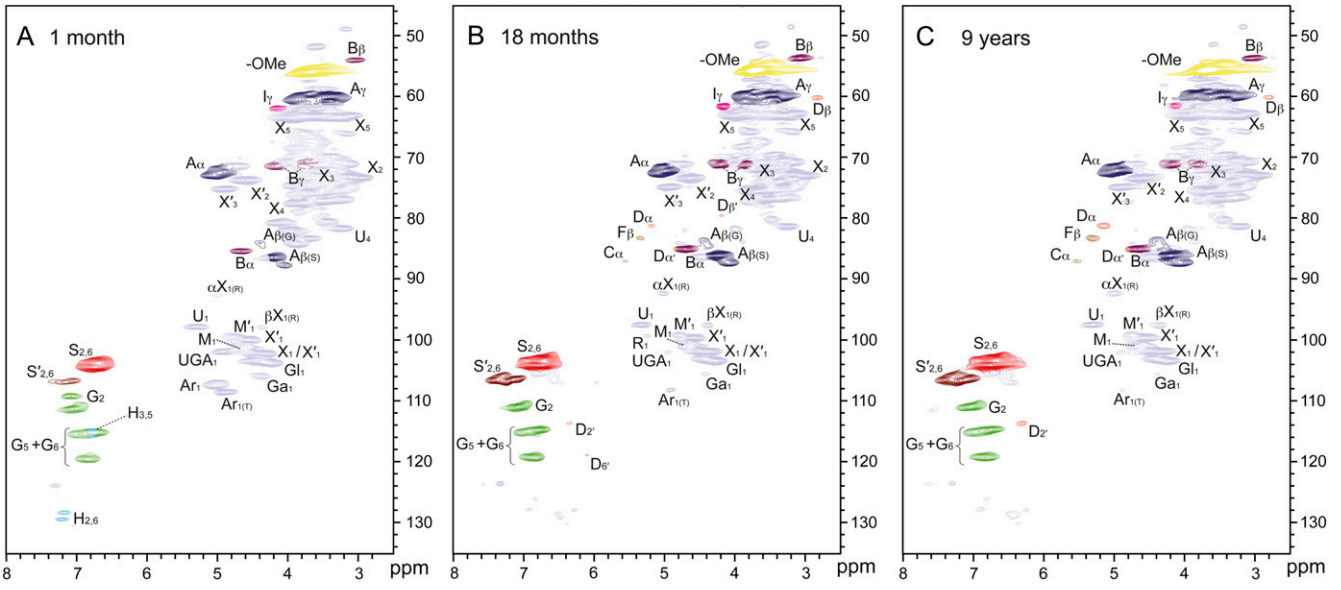

Figure 3. HSQC NMR spectra (δ_C/δ_H 45–135/2.5-8.0 ppm) of the *E. globulus* wood samples at different growth stages after forming a gel in DMSO-d_6:pyridine-d_5 (4:1). See Table III for lignin signal assignment and Figure 5 for the main lignin structures identified. The assignments of the carbohydrate signals are listed in Table IV.

dienone-type (D; 1%–5%) units. The conventional open *β*-1′ structures (E; Lundquist, 1987), which were observed only in the MWL samples, ranged from 1% to 2%.

Some interesting information could be obtained from the wood NMR data. First, it is clear that the changes in monolignol availability during growth influence not only the unit composition but also affect the abundances of some interunit linkages. For example, despite the relative percentage of the *β*-*O*-4′ linkages remaining relatively constant with growth, their abundances per aromatic unit slightly increases (from 46 to 50 linkages per 100 aromatic units), and the same happens with the *β*-*β*′ resinol-type structures (which increase from 10 to 12 linkages per 100 aromatic units), probably as a consequence of the increase of S units. Interestingly, the ratio between the abun-

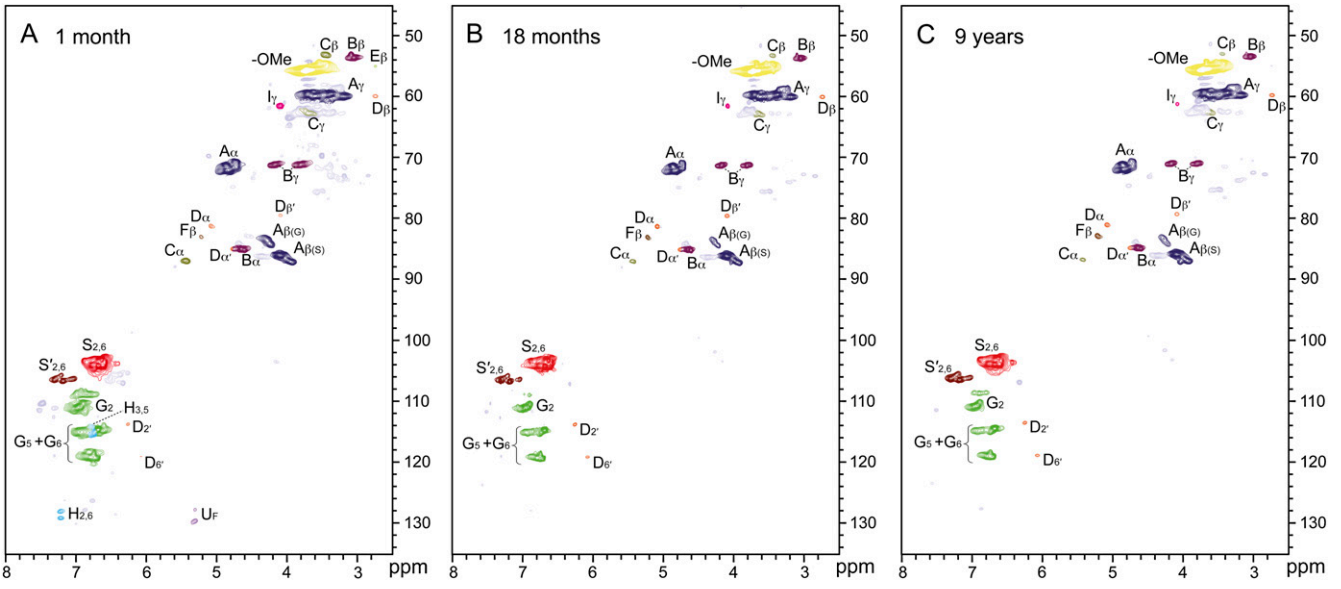

Figure 4. HSQC NMR spectra (δ_C/δ_H 45–135/2.5-8.0 ppm) of the MWLs isolated from the *E. globulus* wood samples at different growth stages. See Table III for lignin signal assignment and Figure 5 for the main lignin structures identified. Olefinic cross-signals of unsaturated fatty acid structures (U_F) were also identified.

Table III. *Assignments of the lignin ^{13}C-^{1}H correlation signals in the HSQC spectra of E. globulus wood at the different growth stages and their isolated MWLs*

Labels	δ_C/δ_H	Assignment
	ppm	
C_β	53.5/3.46	C_β-H_β in phenylcoumaran substructures (C)
B_β	53.5/3.06	C_β-H_β in resinol substructures (B)
E_β	55.0/2.75	C_β-H_β in β-1′ substructures (E)
-OMe	55.6/3.73	C-H in methoxyls
A_γ	59.4/3.40 and 3.72	$C_\gamma H_\gamma$ in β-*O*-4′ substructures (A)
D_β	59.6/2.75	C_β-H_β in spirodienone substructures (D)
I_γ	61.3/4.09	C_γ-H_γ in cinnamyl (sinapyl/coniferyl) alcohol end groups (I)
C_γ	62.5/3.72	C_γ-H_γ in phenylcoumaran substructures (C)
B_γ	71.0/3.83 and 4.19	C_γ-H_γ in resinol substructures (B)
A_α	71.7/4.86	C_α-H_α in β-*O*-4′ substructures (A)
$D_{\beta'}$	79.3/4.11	$C_{\beta'}$-$H_{\beta'}$ in spirodienone substructures (D)
D_α	81.2/5.09	$C_\alpha H_\alpha$ in spirodienone substructures (D)
$A_{\beta(G)}$	83.5/4.28	C_β-H_β in β-*O*-4′ linked to a G unit (A)
F_β	83.8/5.23	C_β-H_β in oxidized (C_α=O) β-*O*-4′ substructures (F)
B_α	84.8/4.67	C_α-H_α in resinol substructures (B)
$D_{\alpha'}$	84.8/4.75	$C_{\alpha'}H_{\alpha'}$ in spirodienone substructures (D)
$A_{\beta(S)}$	85.8/4.11	C_β-H_β in β-*O*-4′ linked to a S unit (A)
C_α	86.8/5.46	C_α-H_α in phenylcoumaran substructures (C)
$S_{2,6}$	103.8/6.69	$C_{2,6}$-$H_{2,6}$ in etherified syringyl units (S)
$S'_{2,6}$	106.6/7.32 and 7.19	$C_{2,6}$-$H_{2,6}$ in oxidized (C_α=O) phenolic syringyl units (S′)
G_2	110.9/6.99	C_2-H_2 in guaiacyl units (G)
$D_{2'}$	113.2/6.27	$C_{2'}H_{2'}$ in spirodienone substructures (D)
$H_{3,5}$	114.9/6.74	$C_{3,5}$-$H_{3,5}$ in *p*-hydroxyphenyl units (H)
G_5/G_6	114.9/6.72 and 6.94; 118.7/6.77	C_5-H_5 and C_6-H_6 in guaiacyl units (G)
$D_{6'}$	118.9/6.09	$C_{6'}H_{6'}$ in spirodienone substructures (D)
$H_{2,6}$	128.0/7.23	$C_{2,6}$-$H_{2,6}$ in *p*-hydroxyphenyl units (H)

dances of β-*O*-4′ and β-β′ resinol-type structures seems to remain more or less constant along lignification. The spirodienone-β-1′ ratio also increased during growth (from 0.8 to 3.2). In contrast, the abundance of phenylcoumaran structures decreases with lignification, which is most probably related to the decrease in G lignin observed. On the other hand, a small but continuous oxidation of the Cα of the lignin side chain (from one to four Cα oxidized β-*O*-4′ linkages per 100 aromatic units) occurs during lignification, probably as a result of wood aging. Finally, the abundance of cinnamyl alcohol end groups decreases with lignification, as also observed by Py-GC-MS.

Hemicellulose Polysaccharides

The HSQC spectra also reveal differences in the carbohydrates present in eucalypt wood after the different growth periods, which are observed in two differentiated regions of the spectra: the aliphatic-oxygenated region and the region corresponding to the anomeric correlations (Fig. 3). The aliphatic-oxygenated region shows strong signals from carbohydrates, including naturally acetylated hemicelluloses. Among them, signals from *O*-acetylated xylans (3-*O*-acetyl-β-D-xylopyranoside [X'_3] and 2-*O*-acetyl-β-D-xylopyranoside [X'_2]) and, at the earlier stages of growth, *O*-acetylated mannans (2-*O*-acetyl-β-D-mannopyranoside [M'_2]) were observed. Other signals in this region correspond to C_2-H_2, C_3-H_3, C_4-H_4, and C_5-H_5 correlations of xylans (β-D-xylopyranoside [X_2, X_3, X_4, and X_5]), which overlap with unassigned cross-signals of other pentose and hexose polysaccharide units (note that crystalline cellulose is practically "invisible" in the HSQC spectra of the wood gels due to its reduced mobility), and the C_4-H_4 correlation for 4-*O*-methyl-α-D-GlcUA (U_4).

However, the main differences are observed in the carbohydrate anomeric region of the spectra, which have been depicted in detail in Figure 6. The main C_1-H_1 correlation signals in this region, which are listed in Table IV, were assigned according to Kim and Ralph (2010), together with some additional references for pectin (Ha et al., 2005; Golovchenko et al., 2007, Hedenström et al., 2008). Cross-signals from arabinans (Ar_1 and $Ar_{1(T)}$), mannans (M_1), galactans (Ga_1), xylans (X_1, $\alpha X_{1(R)}$, and $\beta X_{1(R)}$), and glucans including non-crystalline cellulose (Gl_1), as well as signals from *O*-acetylated mannans and xylans (M'_1 and X'_1) and from the 4-*O*-methyl-α-D-glucuronic (U_1) and galacturonic (UGA_1) acids (the latter forming part of pectin as the methyl ester) are readily apparent and well resolved in this region of the spectra. A small signal of α-Rha (R_1) units was also observed, especially in the 18-month-old wood. Interestingly, the signals of arabinans, mannans, and galactans, which are observed in

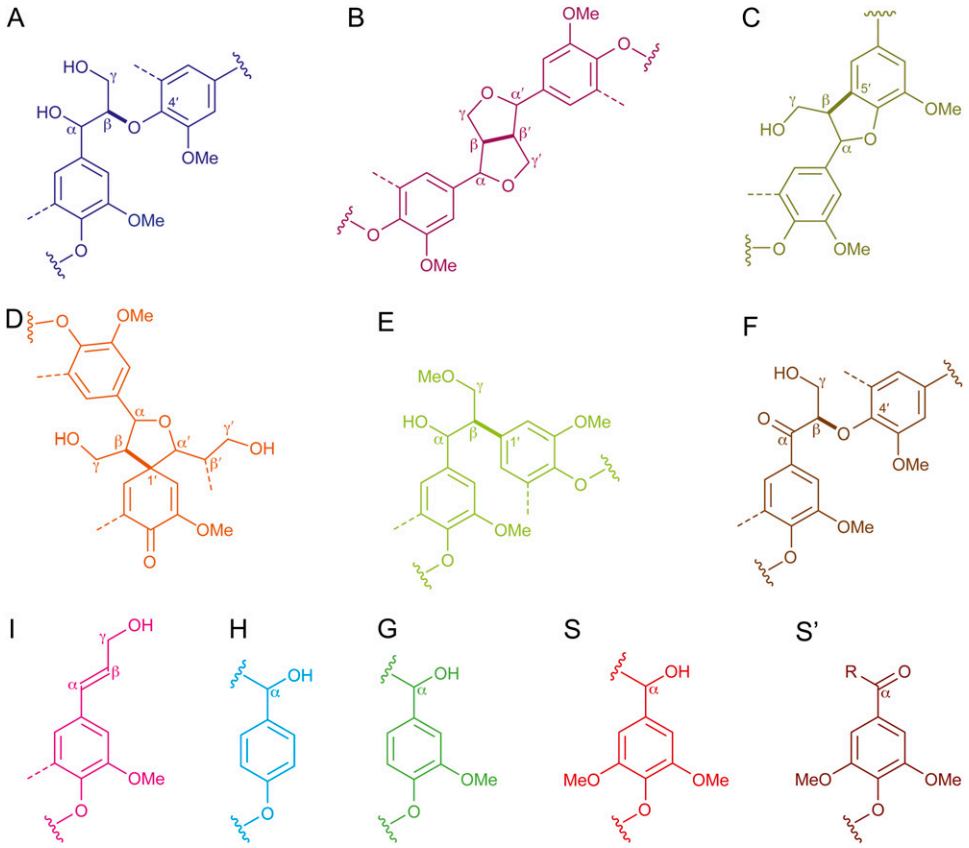

Figure 5. Main substructures present in the *E. globulus* wood lignin during tree growth. A, β-Ether structure formed by β-*O*-4′ linkages. B, Resinol structure including β-β′ linkages. C, Phenylcoumaran structure including β-5′ linkages. D, Spirodienone structure including β-1′ linkages. E, Open β-1′ structure. F, C_α-oxidized β-*O*-4′ structure. I, Cinnamyl alcohol end group. H, *p*-Hydroxyphenyl unit. G, Guaiacyl unit. S, Syringyl unit. S′, Oxidized syringyl unit bearing a carbonyl at Cα.

important amounts in the youngest wood sample, drastically decrease during maturation, while the spectra of the oldest samples are progressively enriched in xylan moieties. Ara and Gal polymers are often associated with pectins. Therefore, the high amounts of these sugars, together with methyl galacturonate (UGA_1 NMR signal), in the youngest wood samples may reflect the higher content of pectin (Coetzze and Wolfaart, 2010). During the subsequent *E. globulus* growth, a positive correlation was found between the increases of lignin S-G ratio and the content of xylan (or the decrease of arabinogalactan), similar to that reported during within-tree variation studies in *E. camaldulensis* and *E. globulus* (Ona et al., 1997).

From the intensities of the corresponding carbohydrate cross-signals in the spectra, it was possible to estimate that one of each two Xyl units bears one acetate group on average occupying the C2 (approximately 60% of units) or C3 (approximately 40%) position (of monoacetylated and diacetylated xylan units). 4-*O*-Methylglucuronic acid xylan branches seem to be less abundant (one for each eight Xyl units on average). Interestingly, the acetylation and 4-*O*-methylglucuronic acid substitution degree in xylan remain constant during growth. These results basically agree with studies on hemicelluloses (xylans and other polysaccharides) isolated from adult eucalypt woods (Shatalov et al., 1999; Evtuguin et al., 2003; Lisboa et al., 2005). Additional studies, required to complete the assignment of the HSQC cross-signals of carbohydrates in the eucalypt wood gels, are outside the scope of this paper. However, the in situ analysis presented here provides a global picture of the composition of the hemicellulose fraction in *E. globulus* wood and its variation during tree growth, without isolating the individual polysaccharides.

Thioacidolysis of the Isolated Lignins

To obtain additional information about the units involved in different linkages of the lignin structure, the MWLs isolated from the *E. globulus* woods at the different growth stages were also studied by thioacidolysis. The degradation products were then subjected to a Raney-nickel desulfurization and the products obtained were analyzed by GC-MS. The chromatogram of the trimethylsilylated products of a representative eucalypt wood MWL sample (from 1-month wood) is shown in Figure 7. The compounds were identified according to previously reported mass spectra (Lapierre et al., 1991; Saito and Fukushima, 2005; Rencoret et al., 2008; del Río et al., 2009). The structures of the main compounds identified are shown in Figure 8, and their mass spectral data are summarized in Table VI.

Table IV. *Assignments of the carbohydrate ^{13}C-^{1}H correlation signals in the HSQC spectra of E. globulus wood at the different growth stages*

R, Reducing end; T, terminal (nonreducing).

Labels	δ_C/δ_H	Assignments
	ppm	
X_5	63.2/3.26 and 3.95	C_5-H_5 in β-D-xylopyranoside
M'_2	70.9/5.41	C_2-H_2 in 2-*O*-acetyl-β-D-mannopyranoside
X_2	72.9/3.14	C_2-H_2 in β-D-xylopyranoside
X'_2	73.5/4.61	C_2-H_2 in 2-*O*-acetyl-β-D-xylopyranoside
X_3	74.1/3.32	C_3-H_3 in β-D-xylopyranoside
X'_3	74.9/4.91	C_3-H_3 in 3-*O*-acetyl-β-D-xylopyranoside
X_4	75.6/3.63	C_4-H_4 in β-D-xylopyranoside
U_4	81.4/3.22	C_4-H_4 in 4-*O*-methyl-α-D-GlcUA
Anomeric correlations (C_1-H_1)		
$\alpha X_{1(R)}$	92.5/5.02	α-D-Xylopyranoside (R) [α-D-glucopyranoside (R)]
$\beta X_{1(R)}$	97.7/4.39	β-D-Xylopyranoside (R) [β-D-glucopyranoside (R)]
U_1	97.7/5.32	4-*O*-Methyl-α-D-GlcUA
M'_1	99.3/4.78	2-*O*-Acetyl-β-D-mannopyranoside
R_1	99.3/5.25	(1→2)-α-D-Rhamnopyranoside
X'_1	99.8/4.58	2-*O*-Acetyl-β-D-xylopyranoside
M_1	101.2/4.69	(1→4)-β-D-Mannopyranoside
UGA_1	101.7/4.94	Methyl(1→4)-α-D-galacturonate
X_1-X'_1	102.1/4.38	β-D-Xylopyranoside + 3-*O*-acetyl-β-D-xylopyranoside
Gl_1	103.3/4.41	(1→4)-β-D-Glucopyranoside
Gl_1	103.6/4.30	(1→3)-β-D-Glucopyranoside + (1→6)-β-D-glucopyranoside
Ga_1	105.6/4.40	(1→4)-β-D-Galactopyranoside
Ar_1	107.3/5.05	α-L-Arabinofuranoside
$Ar_{1(T)}$	108.3/4.91	α-L-Arabinofuranoside (T)

The yield of thioacidolysis monomers increased from the 1-month to the 9-year samples (1,450–2,920 μmol g^{-1}). The low amounts of monomers released from the 1-month sample were probably due to the presence of cutin-like material coextracted or chemically bound to the lignin, as shown by NMR, whose presence was especially high in this MWL sample. The molar composition of the H, G, and S thioacidolysis monomers in the different MWLs is provided in Table VII. It showed a predominance of S over G units in the etherified eucalypt lignin and the nearly complete absence of H units. The abundances of S units in the etherified lignin (over 80%–87%) are higher than in the total lignin, as shown by NMR (56%–76%) and Py-GC-MS (55%–75%) analyses, confirming that the ether-linked lignin is enriched in S units. Possibly, because of

Table V. *Lignin structural characteristics from integration of ^{13}C-^{1}H correlation signals in the HSQC spectra of whole E. globulus wood at different growth stages and their MWLs*

Characteristics include abundance of side chains forming different interunit linkages (A–F) and cinnamyl alcohol end groups (I) per 100 aromatic units (and as percentage of total side chains) as well as H, G, and S contents.

Characteristics	1 Month		18 Months		9 Years	
	Wood	MWL	Wood	MWL	Wood	MWL
Linkages (% side chains involved)						
β-*O*-4′ aryl ether (A)	46 (72)	51 (68)	50 (72)	51 (69)	50 (69)	50 (69)
Resinol (B)	10 (17)	13 (18)	12 (18)	14 (19)	12 (16)	14 (19)
Phenylcoumaran (C)	3 (4)	4 (5)	1 (2)	2 (3)	1 (2)	1 (1)
Spirodienones (D)	1 (1)	2 (3)	2 (3)	3 (4)	4 (5)	3 (5)
β-1′ structures (E)	0 (0)	1 (2)	0 (0)	1 (1)	0 (0)	1 (1)
β-*O*-4′ oxidized at Cα (F)	1 (1)	1 (1)	2 (2)	3 (3)	4 (5)	2 (4)
Cinnamyl alcohol end groups (I)	3 (5)	2 (3)	2 (3)	1 (1)	2 (3)	1 (1)
Lignin units (%)						
H	5	2	0	0	0	0
G	41	42	26	27	23	24
S	53	56	74	73	77	76

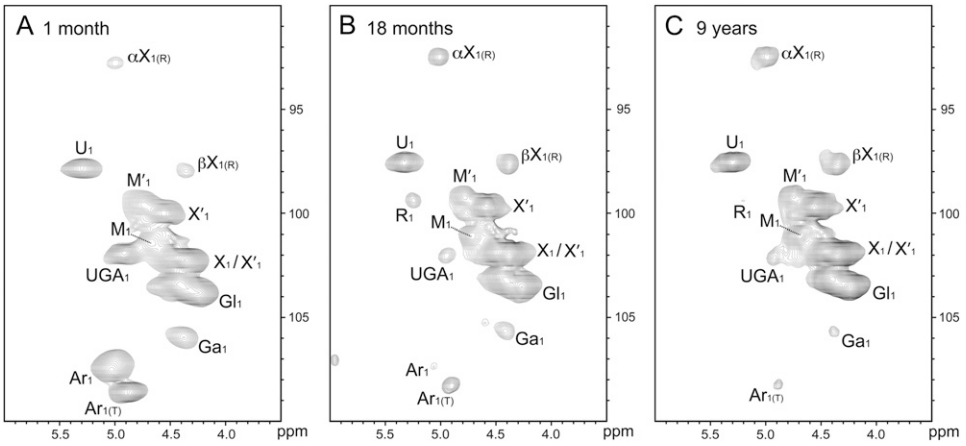

Figure 6. Carbohydrate anomeric regions (δ_C/δ_H 90–110/3.5-6.0 ppm) of HSQC NMR spectra of the *E. globulus* wood samples at different growth stages after forming a gel in DMSO-d_6:pyridine-d_5 (4:1). The assignments of the carbohydrate signals are listed in Table IV.

this high abundance of S units in etherified lignin, no further enrichment was observed in the lignins isolated during tree growth.

The dimers recovered after thioacidolysis provide information on the various carbon-carbon and diaryl ether linkages, referred to as the "condensed" bonds (including 5-5′, 4-*O*-5′, *β*-1′, *β*-5′, and *β*-*β*′; Lapierre et al., 1991, 1995). The relative molar percentages of the different dimers released from the MWLs are shown in Table VIII. The main dimers obtained were of 5-5′ (dimers 5–7), 4-*O*-5′ (8 and 10), *β*-1′ (9, 11, 13, 16, 18, and 26), *β*-5′ (12, 14, 17, and 23), *β*-*β*′ tetralin (15, 19–22, and 25), and phenylisochroman (24 and 27–29; including *β*-1′/*α*-*O*-*α*′ bonds) types (Fig. 8).

The compounds with *β*-*β*′ (tetralin) structures were the most prominent dimers released, accounting from 39% to 52% of the total identified dimers. The high proportion of tetralin-type dimers was in agreement with the high amounts of *β*-*β*′ resinol substructures observed by 2D-NMR. Interestingly, the relative abundances of the tetralin dimers, with respect to the other condensed structures, increase with lignification. More interestingly, most of the *β*-*β*′ dimers released from the different eucalypt lignins were of syringaresinol type, pinoresinol being completely absent, and the G-S resinol structure appearing only in trace amounts (Table VIII). The fact that *β*-*β*′ resinol structures are made almost exclusively of S units explains their increase during lignification due to the parallel increase of S units. The relative abundances of the *β*-1′ dimers were anomalously prominent (around 26% of the total dimeric structures) in comparison with other lignins (Lapierre et al., 1995; Ralph et al., 2004a). Although the total relative abundance of *β*-1′ dimers

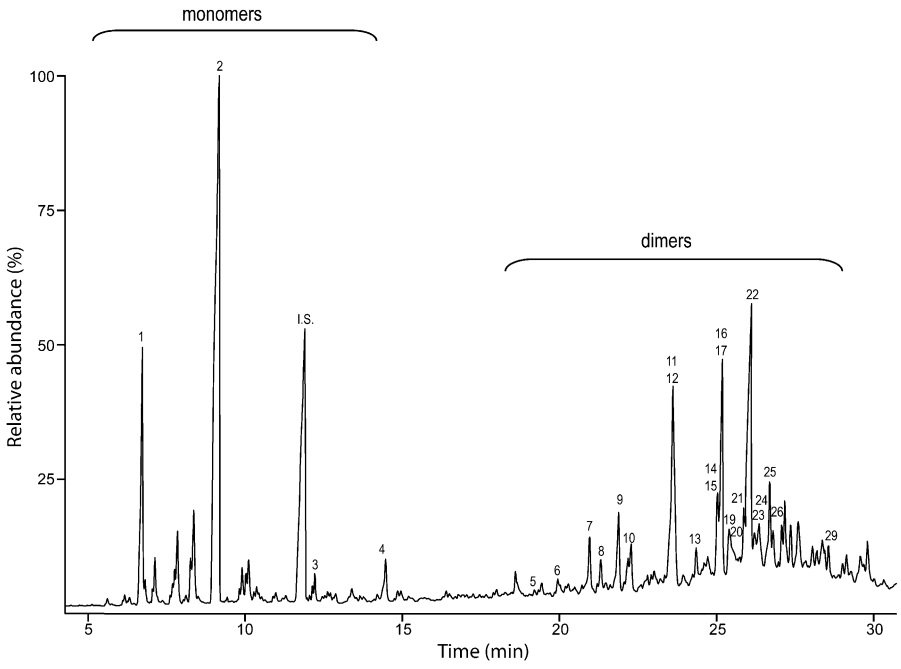

Figure 7. Chromatogram of the thioacidolysis degradation products (after Raney-nickel desulfurization) of a representative MWL from *E. globulus* wood (at 1 month of growth) as trimethylsilyl derivatives. The numbers refer to the compounds (monomers and dimers) listed in Table VI, and the corresponding chemical structures are shown in Figure 8. I.S. refers to octadecane used as an internal standard.

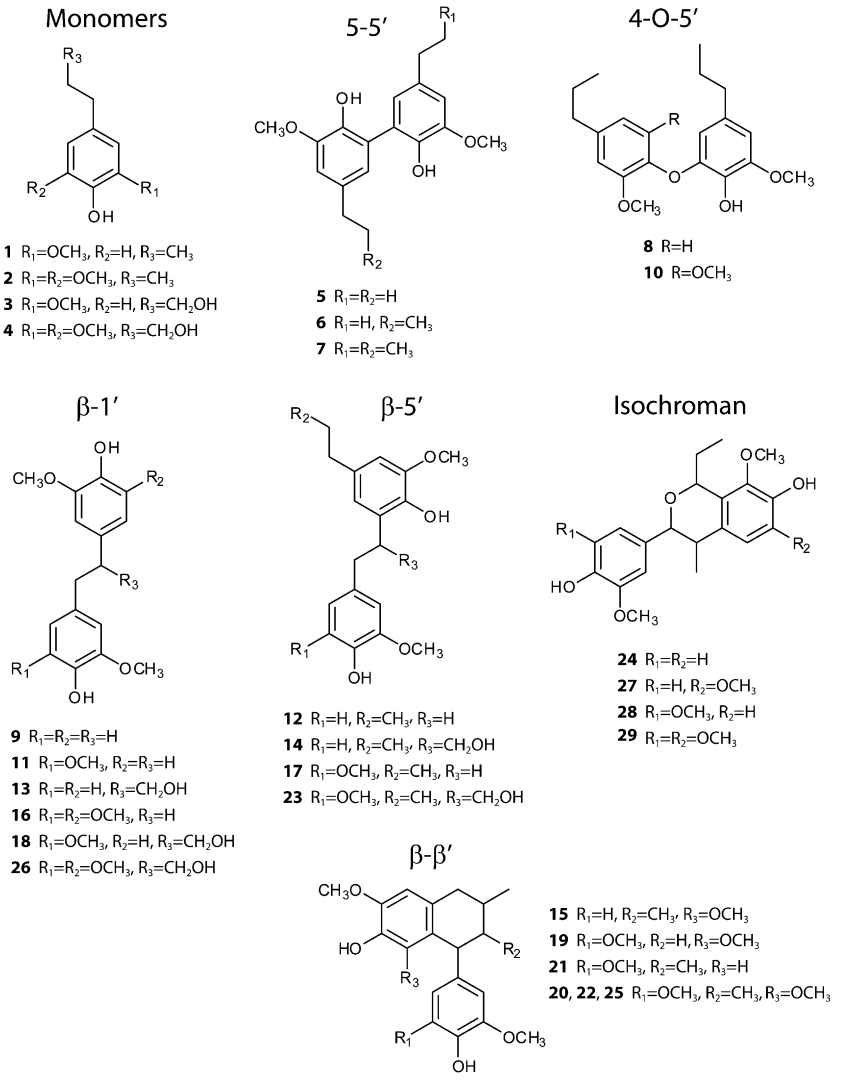

Figure 8. Structures of monomeric and main dimeric compounds obtained after thioacidolysis and Raney-nickel desulfurization of the MWLs isolated from the *E. globulus* wood samples at different growth stages. All mass spectral data of the compounds (as trimethylsilyl derivatives) are listed in Table VI.

was not modified during maturation, the distribution among the different dimeric structures changed, with an increase of structures having two S units, in agreement with the parallel enrichment of S lignin. The *β*-5′ dimers were also released in important amounts from the different MWLs (ranging from 20% to 11% of total dimeric structures) and, in agreement with the HSQC spectra, their abundances decrease with maturation, paralleling the decrease of G units. The 5-5′ dimeric structures, which are considered mostly as being degradation products of dibenzodioxocins and which could not be detected in the HSQC spectra, were found in very small amounts in all the samples (ranging from 2% to 5% of all dimeric compounds), and their content also decreased with maturation, paralleling the decrease of G units. Finally, some trimeric compounds were identified among the thioacidolysis degradation products as being formed by addition to the *β*-*β*′ tetralin dimers described previously (compounds 20, 22, and 25) of a G lignin unit linked by a 4-*O*-5′ ether bond (S-*β*-*β*′-S′-4′-*O*-5′′-G′′ trimers). Three isomers of this trimeric structure, which were previously reported in *Eucalyptus* wood (Rencoret et al., 2008), were detected, as also occurred with the corresponding dimers, and their relative abundances also increased during growth due to the progressive enrichment of S lignin units.

CONCLUSION

This study reports, to our knowledge for the first time by in situ analyses, how the composition and structure of lignin and hemicelluloses in *E. globulus* wood change during plant growth. This was possible by the use of Py-GC-MS, which gives information about the H-G-S composition of the lignin in woods, and by a very recent spectroscopic methodology that combines the high resolution of 2D-NMR with spectra acquisition of the whole wood at the gel stage (by "swelling" in DMSO-d_6:pyridine-d_5 [4:1]), thus enabling the simultaneous analysis of both types of

Table VI. *Identification and mass spectral fragments of the compounds (silylated monomers and dimers) released after thioacidolysis and Raney-nickel desulfurization of MWLs from the different E. globulus woods analyzed, whose structures are depicted in Figure 8*

Linkage type and molecular weight (MW) are indicated, in addition to main mass fragments (the base peaks are underlined). *m/z*, Mass-to-charge ratio.

Compound	Linkage	Fragments	MW
		m/z	
Monomers			
1	G	238, 223, 209, 179, 73	238
2	S	268, 253, 239,238, 209	268
3	G-OH	326, 311, 236, 206, 179	326
4	S-OH	356, 341, 240	356
Dimers			
5	5-5′ (G-G)	446, 431, 417, 416, 73	446
6	5-5′ (G-G)	460, 445, 431, 430, 73	460
7	5-5′ (G-G)	474, 459, 445, 444, 385, 357, 73	474
8	4-*O*-5′ (G-G)	402, 387, 373, 372, 357, 343, 73	402
9	*β*-1′ (G-G)	418, 209, 179, 73	418
10	4-*O*-5′ (G-S)	432, 417, 403, 73	432
11	*β*-1′ (G-S)	448, 433, 239, 209, 179, 73	448
12	*β*-5′ (G-G)	460, 445, 251, 236, 209, 207,179, 73	460
13	*β*-1′ (G-G, -OH)	520, 505, 417, 311, 223, 209, 179, 149, 73	520
14	*β*-5′ (G-G, -OH)	562, 472, 352, 263, 209, 191, 73	562
15	*β*-*β*′ (G-S)	502, 306, 269, 239, 209, 73	502
16	*β*-1′ (S-S)	478, 463, 239, 209, 73	478
17	*β*-5′ (G-S)	490, 239, 209, 73	490
18	*β*-1′ (G-S, -OH)	550, 535, 341, 73	550
19	*β*-*β*′ (S-S)	518, 503, 489, 488, 292, 73	518
20	*β*-*β*′ (S-S)	532, 517, 502, 445, 306, 291, 275, 73	532
21	*β*-*β*′ (G-S)	502, 487, 472, 415, 276, 73	502
22	*β*-*β*′ (S-S)	532, 517, 502, 445, 306, 291, 275, 73	532
23	*β*-5′ (G-S, -OH)	592, 502, 472, 239,209, 191, 73	592
24	*β*-1′/*α*-*O*-*α*′ (G-G)	488, 473, 459, 279, 251, 209, 73	488
25	*β*-*β*′ (S-S)	532, 517, 502, 445, 306, 291, 275, 73	532
26	*β*-1′ (S-S, -OH)	580, 565, 341, 239, 209, 73	580
27	*β*-1′/*α*-*O*-*α*′ (G-S)	518, 503, 489, 309, 239, 209, 73	518
28	*β*-1′/*α*-*O*-*α*′ (S-G)	518, 503, 489, 279, 251, 239, 209, 73	518
29	*β*-1′/*α*-*O*-*α*′ (S-S)	548, 533, 519, 309, 278, 281, 239, 209, 73	548

polymers without the problems often associated with isolation (such as low yield, structural modification, and the presence of contaminating molecules).

The data obtained indicated that not only the lignin content increases with growth but that its composition changes with maturation, the order of monolignol deposition being H, G, and then S at a late stage. The enrichment of S lignin with respect to G and H lignin during lignification also affects the abundance of the different interunit linkages forming the lignin structure. Thus, a decrease of *β*-5′ phenylcoumaran and 5-5′ biphenyl substructures occurred during lignification, paralleling the decrease in G units, and a small increase of *β*-*O*-4′ alkyl-aryl ether substructures was produced, paralleling the enrichment of S units. *β*-*O*-4′ alkyl-aryl ether are the major substructures in eucalypt lignin (69%–72% of side chains) together with *β*-*β*′ resinol substructures (16%–19% of side chains), which interestingly were almost exclusively of the syringaresinol type. On the other hand, open *β*-1′ structures were detected in addition to spirodienones, the abundance of the latter increasing during growth. Finally, a small but continuous oxidation of the C*α* of the lignin side chain, together with a decrease of cinnamyl alcohol end groups, was also observed as lignification proceeds.

Moreover, significant changes in hemicellulose during eucalypt growth were also shown by the HSQC spectra of the wood gels, including increases of xylosyl (which appeared 50% acetylated) and 4-*O*-methylglucuronosyl cross-signals, and strong decreases of those of arabinosyl, galactosyl, and methyl galacturonosyl units (the latter originating from pectin-like polymers). Although more work is required for a complete as-

Table VII. *Relative molar abundance of etherified monomers after thioacidolysis of the MWLs isolated from the E. globulus wood at different growth stages*

Growth Stage	H	G	S
1 month	0.1	20.1	79.8
18 months	0.1	12.8	87.1
9 years	0.1	18.6	81.3

Table VIII. *Relative molar percentages of the different dimer types (see Table V and Fig. 8) released after thioacidolysis (and Raney-nickel desulfurization) of the MWLs isolated from E. globulus wood at different growth stages*

Growth Stage	5-5′	4-*O*-5′		β-1′			β-5′		β-β′			β-1′/α-*O*-α′		
	GG	GG	SG	GG	SG	SS	GG	SG	GG	SG	SS	GG	SG	SS
1 month	4	3	3	7	7	11	9	11	0	3	42	1	1	1
18 months	3	2	3	4	5	17	4	9	0	1	48	1	1	3
9 years	2	2	4	3	4	19	4	7	0	1	51	1	1	4

signment of all the polysaccharide signals in the wood gels, the results obtained showed that not only changes in lignin structure and composition but also the evolution of polysaccharides during plant growth can be followed in situ (without time-consuming and problematic polymer isolation) by the use of 2D-NMR in combination with other techniques.

MATERIALS AND METHODS

Wood Samples

Samples from a selected *Eucalyptus globulus* clone (334-1-AR) at different stages of growth (1 month, 18 months, and 9 years) were provided by the Grupo Empresarial ENCE pulp mill in Pontevedra, Spain, as representative of clonal plantation trees used for paper pulp production. Whole stems of 1-month-old plants, and previously debarked 18-month-old and 9-year-old eucalypt wood chips, were air dried and milled using an IKA cutting mill. The milled samples were successively extracted with acetone in a Soxhlet apparatus for 8 h and then with hot water (3 h at 100°C). Klason lignin was estimated as the residue after sulfuric acid hydrolysis of the preextracted material according to Tappi procedure T222 om-88 (Tappi, 2004). The protein content in the Klason lignin was determined from the nitrogen content (Kjeldahl method) using a 6.25 factor (Darwill et al., 1980). The acid-soluble lignin was determined at 205 nm after the insoluble lignin was filtered off.

Monosaccharide composition of the above wood hydrolysate was determined using a Dionex HPLC system (ICS 3000) equipped with a Dionex AS autosampler, a GP40 gradient pump, an anion-exchange column (Dionex CarboPac PA1), an ED40 electrochemical detector, and different monosaccharide standards. The total uronic acids in the hydrolysate were measured colorimetrically at 520 nm (Blumenkrantz and Asboe-Hansen, 1973). The distribution of amorphous (hemicellulose) and crystalline (cellulose) glucan was calculated by treating the wood with a weak acid, trifluoroacetic acid, and analyzing the hemicellulose sugars, as alditol acetates, by GC-MS with inositol as an internal standard (Albersheim et al., 1967). The residue was washed with the Updegraff (1969) reagent, stripped of further hemicelluloses and amorphous glucan, and totally hydrolyzed with sulfuric acid (Selvendran and O'Neill, 1987), and Glc was quantified by the anthrone assay. Ash content was estimated as the residue after 6 h at 575°C. Two or three replicates were used for each sample.

MWL Isolation

The MWLs were obtained according to the classical procedure (Björkman, 1956). Extractive-free ground wood (prepared as above) was finely ball milled in a Retsch PM100 planetary mill (50 h at 300 rpm for 30 g of wood) using a 500-mL agate jar and agate ball bearings (20 × 20 mm). The milled wood was submitted to an extraction (4× 24 h) with dioxane:water (9:1, v/v; 5–10 mL solvent g^{-1} milled wood). The solution was centrifuged, and the supernatant was evaporated at 40°C under reduced pressure. The residue obtained (raw MWL) was redissolved in acetic acid:water (9:1, v/v; 20 mL solvent g^{-1} raw MWL). The solution was then precipitated into water, and the residue was separated by centrifugation, milled in an agate mortar, and dissolved in 1,2-dicloromethane:ethanol (1:2, v/v). The mixture was then centrifuged to eliminate the insoluble material. The resulting supernatant was precipitated into diethyl ether, and the obtained residue was separated by centrifugation. This residue was then resuspended in petroleum ether and centrifuged again to obtain the purified MWL, which was dried under a current of N_2. The final yields ranged from 10% to 15% based on the Klason lignin content of wood.

Py-GC-MS

Pyrolysis of the different woods and their MWL samples (approximately 100 μg) was performed with a 2020 microfurnace pyrolyzer (Frontier Laboratories) connected to an Agilent 6890 GC-MS system equipped with a DB-1701 fused-silica capillary column (30 m × 0.25 mm i.d., 0.25-μm film thickness) and an Agilent 5973 mass selective detector (electron impact at 70 eV). The pyrolysis was performed at 500°C. The GC oven temperature was programmed from 50°C (1 min) to 100°C at 30°C min^{-1} and then to 290°C (10 min) at 6°C min^{-1}. Helium was the carrier gas (1 mL min^{-1}). The compounds were identified by comparing their mass spectra with those of the Wiley and National Institute of Standards and Technology libraries and those reported in the literature (Faix et al., 1990; Ralph and Hatfield, 1991). Peak molar areas were calculated for the lignin degradation products, the summed areas were normalized, and the data for two repetitive analyses were averaged and expressed as percentages. No attempt was made to calculate the response factor for every single compound released. However, for most of the lignin-derived phenols, the response factors were nearly identical (Bocchini et al., 1997), with the exception of vanillin, but this was a minor peak here.

2D-NMR Spectroscopy

For the NMR of the whole wood, around 100 mg of finely divided (ball-milled) extractive-free wood samples was swollen in DMSO-d_6:pyridine-d_5 (4:1, v/v), according to the method developed by Kim and Ralph (2010). In the case of the MWL, around 40 mg of MWL was dissolved in 0.75 mL of DMSO-d_6.

2D-NMR HSQC spectra were recorded at 25°C on a Bruker AVANCE 500-MHz spectrometer fitted with a cryogenically cooled 5-mm gradient probe with inverse geometry using Bruker's standard pulse sequence "hsqcetgpsisp2.2" (i.e. with adiabatic pulses). The spectral widths were 5,000 and 25,154 Hz for the ^1H and ^{13}C dimensions, respectively. The number of collected complex points was 1,000 for the ^1H dimension (acquisition time, 200 ms), with a recycle delay of 500 ms. The number of transients was 100, and 400 time increments were recorded in the ^{13}C dimension (for an F1 acquisition time of 8 ms). The $^1J_{CH}$ used was 145 Hz. Processing used typical matched Gaussian apodization in ^1H (F2) and a squared cosine bell in ^{13}C (F1). Prior to Fourier transformation, the data matrices were zero filled up to 1,024 points in the ^{13}C dimension. The central solvent peak was used as an internal reference (δ_C/δ_H 39.5/2.49).

A semiquantitative analysis of the integrals of the HSQC correlation contour intensities was performed (Heikkinen et al., 2003; Ralph et al., 2006; Zhang and Gellerstedt, 2007). Integration was performed separately for the different regions of the spectra. In the aliphatic oxygenated region, the various interunit linkages were estimated from C_α-H_α correlations, except for structures E and F described below, where C_β-H_β correlations were used, and structure I, where C_γ-H_γ correlations were used, and the relative abundances of side chains involved in different substructures and terminal structures were calculated (with respect to total side chains). In the aromatic region, ^{13}C-^1H correlations from the different lignin units were used to estimate the H-G-S composition and the S-G ratio.

Thioacidolysis and Raney-Nickel Desulfurization

Thioacidolysis of 5-mg samples of MWL was performed as described by Rolando et al. (1992) using 0.2 M BF_3 etherate in dioxane:ethanethiol (8.75:1).

The reaction products were extracted with CH_2C1_2, dried, and concentrated. Two-hundred microliters of the CH_2Cl_2 solution containing the thioacidolysis products was desulfurized as described by Lapierre et al. (1991). GC-MS analyses were performed in a Varian Star 3400 coupled to an ion-trap detector (Varian Saturn 2000) using a DB-5HT fused-silica capillary column from J&W Scientific (30 m × 0.25 mm i.d., 0.1-μm film thickness). The temperature was programmed from 50°C to 110°C at 30°C min^{-1} and then to 320°C (13 min) at 6°C min^{-1}. The injector and transfer line were at 300°C; the injector was programmed from 120°C (0.1 min) to 380°C at 200°C min^{-1}. Helium was the carrier gas (2 mL min^{-1}), and octadecane was used as an internal standard. Dimer identification was based on previously reported mass spectra (Lapierre et al., 1991; Saito and Fukushima 2005; Rencoret et al., 2008; del Río et al., 2009) and mass fragmentography.

ACKNOWLEDGMENTS

Javier Romero (Grupo Empresarial ENCE) is acknowledged for providing the wood samples, Cliff Foster (Great Lakes Bioenergy Research Center [Michigan State University] cell wall analytical facility) for sugar and cellulose analysis, and Sasikumar Elumalai (University of Wisconsin Biological Systems Engineering Department) for performing the uronic acid analyses.

Received October 11, 2010; accepted November 22, 2010; published November 23, 2010.

LITERATURE CITED

Albersheim P, Nevins DJ, English PD, Karr A (1967) A method for the analysis of sugars in plant cell-wall polysaccharides by gas-liquid chromatography. Carbohydr Res **5:** 340–345

Ämmälahti E, Brunow G, Bardet M, Robert D, Kilpeläinen I (1998) Identification of side-chain structures in a poplar lignin using three-dimensional HMQC-HOHAHA NMR spectroscopy. J Agric Food Chem **46:** 5113–5117

Balakshin MY, Capanema EA, Chang HM (2008) Recent advances in the isolation and analysis of lignins and lignin-carbohydrate complexes. *In* TQ Hu, ed, Characterization of Lignocellulosic Materials. Blackwell Publishing, Oxford, pp 148–170

Balakshin MY, Capanema EA, Chen CL, Gracz HS (2003) Elucidation of the structures of residual and dissolved pine kraft lignins using an HMQC NMR technique. J Agric Food Chem **51:** 6116–6127

Balakshin MY, Capanema EA, Goldfarb B, Frampton J, Kadla JF (2005) NMR studies on Fraser fir *Abies fraseri* (Pursh) Poir. lignins. Holzforschung **59:** 488–496

Björkman A (1956) Studies on finely divided wood. Part I. Extraction of lignin with neutral solvents. Sven Papperstidn **13:** 477–485

Blumenkrantz N, Asboe-Hansen G (1973) New method for quantitative determination of uronic acids. Anal Biochem **54:** 484–489

Bocchini P, Galletti GC, Camarero S, Martínez AT (1997) Absolute quantitation of lignin pyrolysis products using an internal standard. J Chromatogr A **773:** 227–232

Boerjan W, Ralph J, Baucher M (2003) Lignin biosynthesis. Annu Rev Plant Biol **54:** 519–546

Capanema EA, Balakshin MY, Chen CL, Gratzl JS, Gracz H (2001) Structural analysis of residual and technical lignins by ^{1}H-^{13}C correlation 2D NMR-spectroscopy. Holzforschung **55:** 302–308

Capanema EA, Balakshin MY, Kadla JF (2004) A comprehensive approach for quantitative lignin characterization by NMR spectroscopy. J Agric Food Chem **52:** 1850–1860

Capanema EA, Balakshin MY, Kadla JF (2005) Quantitative characterization of a hardwood milled wood lignin by nuclear magnetic resonance spectroscopy. J Agric Food Chem **53:** 9639–9649

Çetinkol OP, Dibble DC, Cheng G, Kent MS, Knierim B, Auer M, Wemmer DE, Pelton JG, Melnichenko YB, Ralph J, et al (2010) Understanding the impact of ionic liquid pretreatment on eucalyptus. Biofuels **1:** 33–46

Coetzze B, Wolfaart F (2010) Pectic monosaccharides and total pectin content of two *Eucalyptus* spp. *In* 1st Symposium on Biotechnology Applied to Lignocelluloses: LignoBiotech-One. INRA, Reims, France, p 141

Darwill A, McNeil M, Albersheim P, Delmer D (1980) The primary cell walls of flowering plants. *In* N Tolbert, ed, The Biochemistry of Plants. Academic Press, New York, pp 91–162

Déjardin A, Laurans F, Arnaud D, Breton C, Pilate G, Leplé JC (2010) Wood formation in angiosperms. C R Biol **333:** 325–334

del Río JC, Gutiérrez A, Hernando M, Landín P, Romero J, Martínez AT (2005) Determining the influence of eucalypt lignin composition in paper pulp yield using Py-GC/MS. J Anal Appl Pyrolysis **74:** 110–115

del Río JC, Rencoret J, Marques G, Gutiérrez A, Ibarra D, Santos JI, Jiménez-Barbero J, Zhang L, Martínez AT (2008) Highly acylated (acetylated and/or *p*-coumaroylated) native lignins from diverse herbaceous plants. J Agric Food Chem **56:** 9525–9534

del Río JC, Rencoret J, Marques G, Li J, Gellerstedt G, Jiménez-Barbero J, Martínez AT, Gutiérrez A (2009) Structural characterization of the lignin from jute (*Corchorus capsularis*) fibers. J Agric Food Chem **57:** 10271–10281

Deshmukh AP, Simpson AJ, Hadad CM, Hatcher PG (2005) Insights into the structure of cutin and cutan from *Agave americana* leaf cuticle using HRMAS NMR spectroscopy. Org Geochem **36:** 1072–1085

Donaldson LA (2001) Lignification and lignin topochemistry: an ultrastructural view. Phytochemistry **57:** 859–873

Evtuguin DV, Tomás JL, Silva AMS, Neto CP (2003) Characterization of an acetylated heteroxylan from Eucalyptus globulus Labill. Carbohydr Res **338:** 597–604

Faix O, Meier D, Fortmann I (1990) Thermal degradation products of wood: a collection of electron-impact (EI) mass spectra of monomeric lignin derived products. Holz Roh-Werkstoff **48:** 351–354

Fujimoto A, Matsumoto Y, Chang HM, Meshitsuka G (2005) Quantitative evaluation of milling effects on lignin structure during the isolation process of milled wood lignin. J Wood Sci **51:** 89–91

Golovchenko VV, Bushneva OA, Ovodova RG, Shashkov AS, Chizhov AO, Ovodov YS (2007) Structural study of bergenan, a pectin from *Bergenia crassifolia*. Russian J Bioinorg Chem **33:** 47–56

González-Vila FJ, Almendros G, del Río JC, Martín F, Gutiérrez A, Romero J (1999) Ease of delignification assessment of different *Eucalyptus* wood species by pyrolysis (TMAH)-GC/MS and CP/MAS 13C-NMR spectrometry. J Anal Appl Pyrolysis **49:** 295–305

Guerra A, Filpponen I, Lucia LA, Saquing C, Baumberger S, Argyropoulos DS (2006) Toward a better understanding of the lignin isolation process from wood. J Agric Food Chem **54:** 5939–5947

Ha MA, Viëtor RJ, Jardine GD, Apperley DC, Jarvis MC (2005) Conformation and mobility of the arabinan and galactan side-chains of pectin. Phytochemistry **66:** 1817–1824

Hedenström M, Wiklund S, Sundberg B, Edlund U (2008) Visualization and interpretation of OPLS models based on 2D NMR data. Chemom Intell Lab Syst **92:** 110–117

Heikkinen S, Toikka MM, Karhunen PT, Kilpeläinen IA (2003) Quantitative 2D HSQC (Q-HSQC) via suppression of J-dependence of polarization transfer in NMR spectroscopy: application to wood lignin. J Am Chem Soc **125:** 4362–4367

Higuchi T (1997) Biochemistry and Molecular Biology of Wood. Springer-Verlag, London

Hu Z, Yeh TF, Chang HM, Jameel H (2006) Elucidation of the structure of cellulolytic enzyme lignin. Holzforschung **60:** 389–397

Ibarra D, Chávez MI, Rencoret J, del Río JC, Gutiérrez A, Romero J, Camarero S, Martínez MJ, Jiménez-Barbero J, Martínez AT (2007a) Lignin modification during *Eucalyptus globulus* kraft pulping followed by totally chlorine-free bleaching: a two-dimensional nuclear magnetic resonance, Fourier transform infrared, and pyrolysis-gas chromatography/mass spectrometry study. J Agric Food Chem **55:** 3477–3490

Ibarra D, Chávez MI, Rencoret J, del Río JC, Gutiérrez A, Romero J, Camarero S, Martínez MJ, Jimenez-Barbero J, Martínez AT (2007b) Structural modification of eucalypt pulp lignin in a totally chlorine free bleaching sequence including a laccase-mediator stage. Holzforschung **61:** 634–646

Kim H, Ralph J (2010) Solution-state 2D NMR of ball-milled plant cell wall gels in DMSO-d_6/pyridine-d_5. Org Biomol Chem **8:** 576–591

Kim H, Ralph J, Akiyama T (2008) Solution-state 2D NMR of ball-milled plant cell-wall gels in DMSO-d_6. Bioenergy Res **1:** 56–66

Lapierre C, Pollet B, Monties B (1991) Thioacidolysis of spruce lignin: GC-MS analysis of the main dimers recovered after Raney nickel desulphuration. Holzforschung **45:** 61–68

Lapierre C, Pollet B, Rolando C (1995) New insights into the molecular

architecture of hardwood lignins by chemical degradative methods. Res Chem Intermed **21:** 397–412

Liitiä TM, Maunu SL, Hortling B, Toikka M, Kilpeläinen I (2003) Analysis of technical lignins by two- and three-dimensional NMR spectroscopy. J Agric Food Chem **51:** 2136–2143

Lisboa S, Evtuguin DV, Pascoal Neto C, Goodfellow B (2005) Isolation and structural characterization of polysaccharides dissolved in *Eucalyptus globulus* kraft black liquors. Carbohydr Polym **60:** 77–85

Lundquist K (1987) On the occurrence of β-1 structures in lignin. J Wood Chem Technol **7:** 179–185

Mazumder BB, Nakgawa-izumi A, Kuroda K, Ohtani Y, Sameshima K (2005) Evaluation of harvesting time effects on kenaf bast lignin by pyrolysis-gas chromatography. Ind Crops Prod **21:** 17–24

Ona T, Sonoda T, Ito K, Shibata M (1997) Relationship of lignin content, lignin monomeric composition and hemicellulose composition in the same trunk sought by their within-tree variations in *Eucalyptus camaldulensis* and *E. globulus*. Holzforschung **51:** 396–404

Ralph J, Akiyama T, Kim H, Lu F, Schatz PF, Marita JM, Ralph SA, Reddy MSS, Chen F, Dixon RA (2006) Effects of coumarate 3-hydroxylase down-regulation on lignin structure. J Biol Chem **281:** 8843–8853

Ralph J, Hatfield RD (1991) Pyrolysis-GC-MS characterization of forage materials. J Agric Food Chem **39:** 1426–1437

Ralph J, Landucci LL (2010) NMR of lignins. *In* C Heitner, DR Dimmel, JA Schmidt, eds, Lignin and Lignans: Advances in Chemistry. CRC Press, Boca Raton, FL, pp 137–234

Ralph J, Lundquist K, Brunow G, Lu F, Kim H, Schatz PF, Marita JM, Hatfield RD, Ralph SA, Christensen JH, et al (2004a) Lignins: natural polymers from oxidative coupling of 4-hydroxyphenylpropanoids. Phytochem Rev **3:** 29–60

Ralph J, Marita JM, Ralph SA, Hatfield RD, Lu F, Ede RM, Peng J, Quideau S, Helm RF, Grabber JH, et al (1999) Solution-state NMR of lignin. *In* DS Argyropoulos, ed, Advances in Lignocellulosics Characterization. Tappi Press, Atlanta, pp 55–108

Ralph SA, Ralph J, Landucci L (2004b) NMR Database of Lignin and Cell-Wall Model Compounds. U.S. Forest Products Laboratory, Madison, WI. http://ars.usda.gov/Services/docs.htm?docid=10491 (July 3, 2006)

Rencoret J, Gutiérrez A, del Río JC (2007) Lipid and lignin composition of woods from different eucalypt species. Holzforschung **61:** 165–174

Rencoret J, Marques G, Gutiérrez A, Ibarra D, Li J, Gellerstedt G, Santos JI, Jiménez-Barbero J, Martínez AT, del Río JC (2008) Structural characterization of milled wood lignin from different eucalypt species. Holzforschung **62:** 514–526

Rencoret J, Marques G, Gutiérrez A, Nieto L, Santos JI, Jiménez-Barbero J, Martínez AT, del Río JC (2009) HSQC-NMR analysis of lignin in woody (*Eucalyptus globulus* and *Picea abies*) and non-woody (*Agave sisalana*) ball-milled plant materials at the gel state. Holzforschung **63:** 691–698

Rodrigues J, Meier D, Faix O, Pereira H (1999) Determination of tree to tree variation in syringyl/guaiacyl ratio of *Eucalyptus globulus* wood lignin by analytical pyrolysis. J Anal Appl Pyrolysis **48:** 121–128

Rolando C, Monties B, Lapierre C (1992) Thioacidolysis. *In* SY Lin, CW Dence, eds, Methods in Lignin Chemistry. Springer-Verlag, Berlin, pp 334–349

Saito K, Fukushima K (2005) Distribution of lignin interunit bonds in the differentiating xylem of compression and normal woods of *Pinus thunbergii*. J Wood Sci **51:** 246–251

Selvendran RR, O'Neill MA (1987) Isolation and analysis of cell-walls from plant material. *In* G David, ed, Methods of Biochemical Analysis. John Wiley & Sons, New York, pp 25–153

Shatalov AA, Evtuguin DV, Pascoal Neto C (1999) (2-*O*-(-D-Galactopyranosyl-4-*O*-methyl-(-D-glucurono)-D-xylan from *Eucalyptus globulus* Labill. Carbohydr Res **320:** 93–99

Tappi (2004) TAPPI Test Methods 2004-2005. TAPPI Press, Norcross, GA

Terashima N, Fukushima K, Tsuchiya S (1986) Heterogeneity in formation of lignin. 7. An autoradiographic study on the formation of guaiacyl and syringyl lignin in poplar. J Wood Chem Technol **6:** 495–504

Updegraff DM (1969) Semimicro determination of cellulose in biological materials. Anal Biochem **32:** 420–424

Yokoi H, Ishida Y, Ohtani H, Tsuge S, Sonoda T, Ona T (1999) Characterization of within-tree variation of lignin components in *Eucalyptus camaldulensis* by pyrolysis-gas chromatography. Analyst (Lond) **124:** 669–674

Yokoi H, Nakase T, Ishida Y, Ohtani H, Tsuge S, Sonoda T, Ona T (2001) Discriminative analysis of *Eucalyptus camaldulensis* grown from seeds of various origins based on lignin components measured by pyrolysis-gas chromatography. J Anal Appl Pyrolysis **57:** 145–152

Zhang L, Gellerstedt G (2007) Quantitative 2D HSQC NMR determination of polymer structures by selecting suitable internal standard references. Magn Reson Chem **45:** 37–45